VERSITA

Cent. Eur. J. Chem. • 10(6) • 2012 • 1954-1962
DOI: 10.2478/s11532-012-0121-3

Central European Journal of **Chemistry**

Novel Cu and Cu_2In/aluminosilicate type catalysts for the reduction of biomass-derived volatile fatty acids to alcohols

Research Article

Szabolcs Harnos[1*], György Onyestyák[1], Róbert Barthos[1], Magdalena Štolcová[2], Alexander Kaszonyi[2], József Valyon[1]

[1]*Institute of Materials and Environmental Chemistry, Research Centre for Natural Sciences, Hungarian Academy of Science, Budapest H-1025, Hungary*

[2]*Department of Organic Technology, Slovak University of Technology, Bratislava SK-81237, Slovak Republic*

Received 2 March 2012; Accepted 13 August 2012

Abstract: This work relates to the consecutive reduction of short chain carboxylic acids (volatile fatty acids, VFAs) to alcohols as main products. Acetic acid (AA) was used as a reactant to model the VFAs that can be produced by either thermochemical or biological biomass degradation. The amorphised zeolite supported copper catalysts (Cu/SiAl), especially the In-modified CuIn/SiAl catalysts, showed high hydroconversion activity and selectivity for alcohol, ester and aldehyde. Catalysts containing dispersed copper particles in amorphous aluminosilicate were obtained by dehydrating and H_2-reducing Cu-forms of low-silica synthetic zeolites (A, X, P). The activity of the highly destructed Cu-aluminosilicates was found to depend on the structure of the zeolite precursor. The formation of ethyl acetate could be suppressed by adding water to the AA feed and by modifying the catalyst, *e.g.* by In_2O_3 additive. In the catalysts modified by In_2O_3 additive formation of copper-indium alloy phase (Cu_2In intermetallic compound) was detected resulting in a different selectivity than the one recorded for the Cu/SiAl.

Keywords: *Acetic acid reduction • Cu-zeolites • In_2O_3 doping • Ethanol • Ethyl acetate*

1. Introduction

The technologies used to produce chemicals and fuels on various biomass platforms involve combination of mechanical, chemical, bio- and thermochemical, and separation operations [1-3]. Except for the sugar-to-alcohol route, all biomass conversion processes generate carboxylic acids as intermediates. Acknowledging the need of transportation and other industrial sectors for chemicals, there is a high commercial interest in the selective catalytic hydroconversion of bioacids to alcohols, ethers, and esters. The deep reduction of short chain carboxylic acids and other oxygenates provides gaseous paraffinic hydrocarbons. Because of the need for liquid fuel the selective reduction of these components to alcohols is the most favored.

The alcohols obtained from the volatile fatty acids (VFAs) can be used as chemicals as well as transportation fuel. The low-boiling fraction (up to 150°C) of the distillate of bio-oil, obtained from lignocellulose pyrolysis, contains lower carboxylic acids and aldehydes in relatively high concentration. Fuel alcohol can be obtained by selective reduction of these components. Instead of the less advantageous thermochemical routes, a novel and favorable microbiological destruction /MixAlco/ process is elaborated [4]. In principle, the biogas process is suggested to be stopped after the rapid anaerobic acidogenic digestion stage, which would be followed by the slow methanogenesis step, to produce the VFAs [5,6]. The selective hydrogenation of the fatty acids to alcohols in a continuous flow system, working in vapor phase under mild conditions, seems to be the problem to be solved.

From the early 1930s up to now triglycerides were used mainly to produce fatty alcohols [7]. The technology of fatty alcohols production involves hydrogenation of

* *E-mail: harnos.szabolcs@ttk.mta.hu*

triglycerides over toxic chromium-containing catalysts. Such chromium-promoted copper catalysts permit the selective addition of hydrogen to carbon-oxygen bonds but are relatively inactive in the hydrogenolysis of the carbon-carbon bonds. However, because the use of chromium raises environmental concerns, the current research is focused on developing chromium-free catalysts [8]. Since esters can be reduced with hydrogen more easily than the carboxylic acids [9], the difficulty of the selective fatty acid reduction was circumvented by including an esterification step. Nevertheless, the patent literature describes numerous catalysts for acetic acid (AA) hydrogenation comprising of one or more Group VIII noble metals dispersed on Group III or IV metal oxides. Rachmady and Vannice have recently shown related results in a series of papers describing catalysts carrying platinum on TiO_2, SiO_2, Al_2O_3 and Fe_2O_3 supports [10-14].

Recently, copper exchanged zeolites were reduced by hydrogen and used as catalysts for hydrogenation of octanoic acid, a model reactant. It was shown by X-ray powder diffraction (XRD) that amorphous silica-alumina supporting finely dispersed copper nanoparticles were formed from Cu-forms of low Si/Al-ratio synthetic zeolites (A, X, P). The In_2O_3 additive was shown to increase the activity and selectivity of the supported copper catalyst in the reduction of long chain fatty acids to alcohols [15]. The study presented hereby refers to the application of similar catalyst systems for the selective reduction of the VFAs to alcohols. Acetic acid (AA) has been used as a model reactant in most of the experiments and compared with the conversion of the long chain octanoic acid (OA) to present more detailed studies of the nature of the mono- and bi-metallic catalysts.

2. Experimental procedure

2.1. Catalysts

Copper-zeolites (CuZ), such as zeolite CuA, CuX, CuY and CuP, were prepared from NaA (Baylith), NaX or NaY (products of the late VEB CKB, Bitterfeld-Wolfen, Germany) and NaP (Crosfield Zeocross) powders, respectively. The Cu-forms were obtained by conventional aqueous ion-exchange using Cu(II) acetate (purity >99%, from Merck) solutions. A slurry of zeolite and an aqueous Cu(II) acetate solution, having a liquid to solid weight ratio of about 10, was stirred at room temperature. The amount of Cu^{2+} in the slurry was about equivalent with the ion-exchange capacity of the zeolite. After 8 hours of stirring the solid and the solution were separated and the exchange procedure was repeated using a fresh solution. The solid was separated again, washed three times with distilled water and dried at room temperature. The Cu^{2+} content of three (A, X, P) catalysts was 14-16 wt.% and 7 wt.% Cu^{2+} for zeolite Y which had lower Al or cation content and higher Si/Al ratio (2.6). The Si/Al ratio was very low (approx. 1) in Cu-A, -X and -P zeolites reflecting similar chemical composition. Zeolite A (small pore) and faujasites (zeolite X or Y, large pore) have different frameworks but consist of the same building units (linked truncated octahedra, β-cages). CuP is a small pore zeolite, but with a quite different gismondite skeleton containing different building units. The main chemical characteristics of zeolites are summarized in Table 1.

Table 1. Composition of the zeolites.

Sample	Si/Al	Al	Na	Cu
		mmol g^{-1}		
NaP	0.95	7.31	6.77	-
NaA	1.21	6.58	6.05	-
NaX	1.48	5.80	6.08	-
NaY	2.57	3.12	3.06	-
14CuP	-	6.86	0.12	2.20
16CuA	-	6.11	0.50	2.52
15CuX	-	6.02	1.18	2.39
7CuY	-	3.01	0.87	1.10

Cu(II) acetate was impregnated on an industrial amorphous silica-alumina (SiAl), having a Si to Al ratio of 6.6, to obtain 20Cu/SiAl catalyst with 20 wt.% Cu content. After drying, this impregnated sample was air calcined at 550°C for 3 h to decompose the acetate to copper oxide.

Composite catalysts were prepared by adding indium(III) oxide (99.99% purity, from Aldrich) to the CuZ samples and grinding the mixture in an agate mortar. For comparison, an applied Adkins catalyst was a commercial product obtained from Süd-Chemie AG (consisting of 72 wt.% $CuCr_2O_4$ and 28 wt.% CuO).

For the designation of the prepared catalysts the symbol of the element copper (Cu) is used, followed by the name of the zeolite (A, X, Y, P), such as CuX. Specific samples are distinguished by including the metal content, expressed in weight percent, in the sample designation, such as 14CuP. The various indium-containing CuZ samples are specified by the amount of the admixed In_2O_3, in weight percent, followed by the designation of the CuZ, such as $15In_2O_3$/14CuP, which means a sample obtained by admixing as much indium(III) oxide to zeolite 14CuP, which amounts to 15 wt.% of the Cu-zeolite. The atomic ratio of Cu/In is approx. 2 in this case.

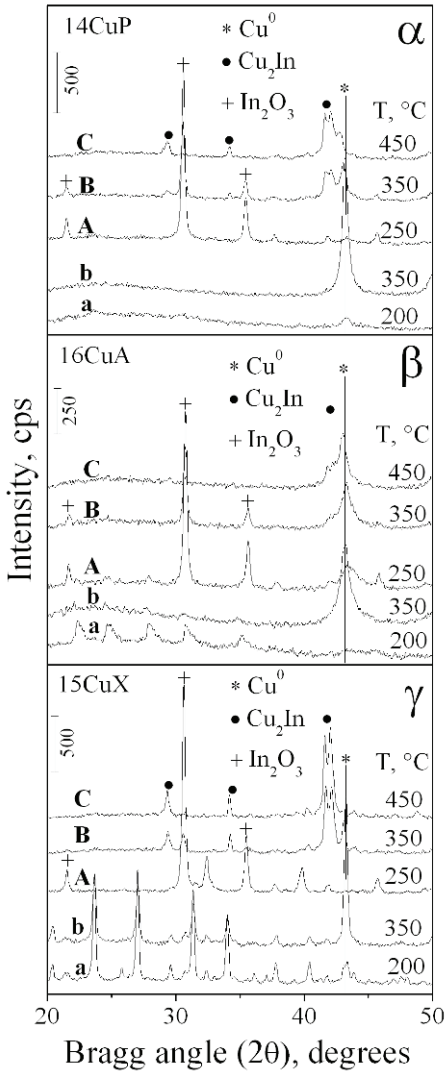

Figure 1. HT-XRD patterns of (α) 14CuP (a, b) and $15In_2O_3$/14CuP (A, B, C) samples treated in H_2 flow at the indicated temperature for half an hour. Similar figures are shown for 16CuA (β) and 15CuX (γ).

2.2. Methods

X-ray patterns were recorded by Philips PW 1810/1870 diffractometer applying monochromatic Cu K_α radiation at elevated temperatures in hydrogen flow using a high-temperature XRD cell (HT-XRD). The mean crystallite size of the copper particles was estimated by the Debye-Scherrer equation.

Nitrogen physisorption measurements were carried out at -196°C using Quantochrome Autosorb 1C instrument for determination of specific surface areas.

The Al, Na and Cu contents of the zeolites were determined by Atomic Absorption Spectroscopy (AAS), using Varian Spectra A20 spectrophotometer, after digesting the zeolite powders in concentrated HF solution.

2.3. Catalytic experiments

The catalytic hydrogenation of AA (96%, from Reanal) and OA (octanoic acid, purity ≥98%, from Aldrich) was carried out in a high pressure fixed bed flow-through reactor at 21 bar total pressure in the temperature range of 300-380°C. The inner diameter of the flow reactor was 16 mm and the height of catalyst bed - 120 mm. The prepared catalyst powders were pressed to pellets without using a binder and applied as catalysts in a form of crashed particles of 0.63-1.00 mm in size. All the catalysts were activated in 230 mL min^{-1} pure hydrogen flow *in situ* in the reactor at 450°C for 1 h prior to using them in reactions. Thereafter the system was cooled down to the desired reaction temperature at which the appropriate feed begun. The reaction was allowed to run one hour at each temperature to attain a steady state. Before taking a sample, the effluent was collected during the second hour, depressurized and cooled to room temperature.

The product mixture, liquid at ambient conditions, was analyzed using a gas chromatograph (Shimadzu 2010) equipped with a flame ionization detector and with a HP-Plot/U capillary column for organic AA products or with a CP-FFAP CB capillary column for OA products. The quantities of water produced were calculated from the oxygen balance. The gaseous reactor effluent was analyzed for CO_2, CO, CH_4 and light hydrocarbons using an on-line gas chromatograph (HP 5890) with a thermal conductivity detector (TCD) on Carboxen 1006 PLOT capillary column.

The results are represented as stacked area graphs. Notice that the distance between two neighboring curves represents the concentration of a given product at a given temperature in weight percent.

3. Results and discussion

3.1. Structural changes in the catalysts

The HT-XRD results suggest that in the catalysts, activated at 450°C in H_2 flow before the reaction of carboxylic acid hydroconversion, all the copper was present in finely dispersed metal nanoparticles (Figs. 1α-1γ). The admixed In_2O_3 could be reduced at higher temperature than the copper ions.

Upon zeolite dehydration and reduction of charge compensating Cu^{2+} cations, the zeolite P and A structure collapsed at temperatures below 250°C (Fig. 1αa and 1βa). Regarding their structural instability towards dehydration and H_2-reduction the zeolites CuP, CuA, and CuX seem to behave similarly, a low level of crystallinity remained (XRD lines from the zeolites disappeared or intensities dropped to a low level). However the degree

of the destruction is significantly different and depends on the original tectonic aluminosilicate skeleton. The reason is that the dehydration of the catalyst containing divalent copper cations, as well as the reduction of these ions with hydrogen, is paralleled by the formation of structurally unstable acidic zeolite forms (H-zeolites). The diffraction line, assigned to the metallic copper phase (Cu^0), appeared only between 250 and 350°C. Thus, the metal nanoparticles were formed only when the zeolite structure had already collapsed or been deeply damaged.

The destructed Cu-zeolite catalysts have specific surface areas of 8 $m^2\ g^{-1}$ for 16CuA, 18 $m^2\ g^{-1}$ for 15CuX, and 30 $m^2\ g^{-1}$ for 14CuP. These surface areas are low in comparison with the 221 $m^2\ g^{-1}$ surface area of the 20Cu/SiAl amorphous industrial aluminosilicate catalyst. There is no simple correlation between the surface area and the hydroconversion activity because, in this relation, the size of copper nanoparticles has also some relevance. The largest copper particles, having an average diameter of 98 nm, are in the 20Cu/SiAl catalyst. In this catalyst the specific surface area of the support is the largest and that of the copper metal is the smallest among all the studied catalysts. The average copper particle size in 16CuA, in 15CuX, in 7CuY and in 14CuP catalysts are 7 nm, 26 nm, 55 nm and 17 nm, respectively. In the stable CuY and the unstable CuX, where in the large pore faujasite framework copper cations have more or less free access to the reducing agent hydrogen and the formed copper atoms can migrate to the surface of the zeolite crystals without a barrier, the average copper particle sizes are larger.

In general, the modification by indium changes the hydrogenation activity of the copper catalyst. An appearance of an intemetallic compound seems to be responsible for the significant change in the catalytic behaviors the new active Cu_2In alloy phase (Fig. 1). XRD patterns of the composite catalyst samples show that above 350°C In_2O_3 lines completely disappear, indicating a total reduction, however upon cooling to room temperature indium metal particles can not be detected (not shown). This final state still differs from the state when small copper particles were not present at all. In^0 diffraction lines can only be detected after cooling to R.T., far below the melting point of the support, which has no copper nanoparticles (not shown). After reduction of the In_2O_3 phase, liquid indium (its melting point being 156.4°C) is formed and spreads over the solid surface. New lines at a bit lower Bragg angles than the most intense line of copper at 43.3° appear in the diffractograms which can be assigned to some kind of Cu-In alloy [16], mainly to Cu_2In phase. This phase was determined using the ICDD database (ICDD number: 42-1475). It can be concluded that: if the catalyst contains enough reduced metallic copper nanoparticles (some are not detectable because of their small size), the total mass of indium reduced at lower temperature can form Cu-In alloy and thus In^0 diffraction lines do not appear after cooling. The shape and intensity of the diffraction lines assigned to Cu_2In phase are different for zeolites X and A or P reflecting a different structure of the precursor. For example, Cu_2In phase is less detectable in the less permeable, more compact (specific surface area of 8 $m^2\ g^{-1}$) destructed CuA sample, where the detectable average copper particle size is the smallest one, 7 nm. The average particle size of Cu_2In nanoparticles practically seems to be equal to monometallic particles.

3.2. Conversion of the carboxylic acids over the base Cu-catalysts

The catalytic activity and selectivity of the prepared catalyst are characterized by the product distribution as function of temperature (see Figs. 2 and 3). Gaseous products (mainly ethane and traces of CH_4, CO and CO_2) were produced only over the industrial amorphous silica-alumina, 20Cu/SiAl catalyst containing 20 wt% of copper (Fig. 3c). Main products formed from AA over all In-free Cu-catalysts were ethanol and ethyl acetate (Figs. 2a-2c and 3b, 3c, and 3C). Almost no acetaldehyde, formed as an intermediate, was detected for Cu catalysts, although it was proven at various experiments, that the acid was converted first to an aldehyde and then to an alcohol. Depending on the reaction conditions fractions of the reactant acid and the product alcohol formed ethyl acetate according to the Fischer esterification mechanism. The change in ethyl acetate concentration indicates that its formation is dependent on both the reactant (acid) and the product (alcohol) concentration decreasing or increasing, respectively.

When converting a longer carbon chain fatty acid, *e.g.* octanoic acid (OA), as a reactant over CuP catalysts [15], an alcohol and its monomolecular dehydrated derivative (octenes in case of OA) are also found as products (Fig. 3a). Neither ether nor ester has been detected as a product of conversion of long chain carboxylic acids. The effects of different alkyl-chain lengths of reactants and of adsorption affinities determining the coverage of the reactant or product compounds on the same active surface result in significant differences in the catalytic activity and the product distribution (compare Figs. 3a and 3b).

With the exception of 16CuA and 7CuY, all other catalysts (Figs. 2b, 3b and 3c) were significantly more active than the commercial chromium-containing Adkins catalyst (Fig. 3C) and show a different selectivity with

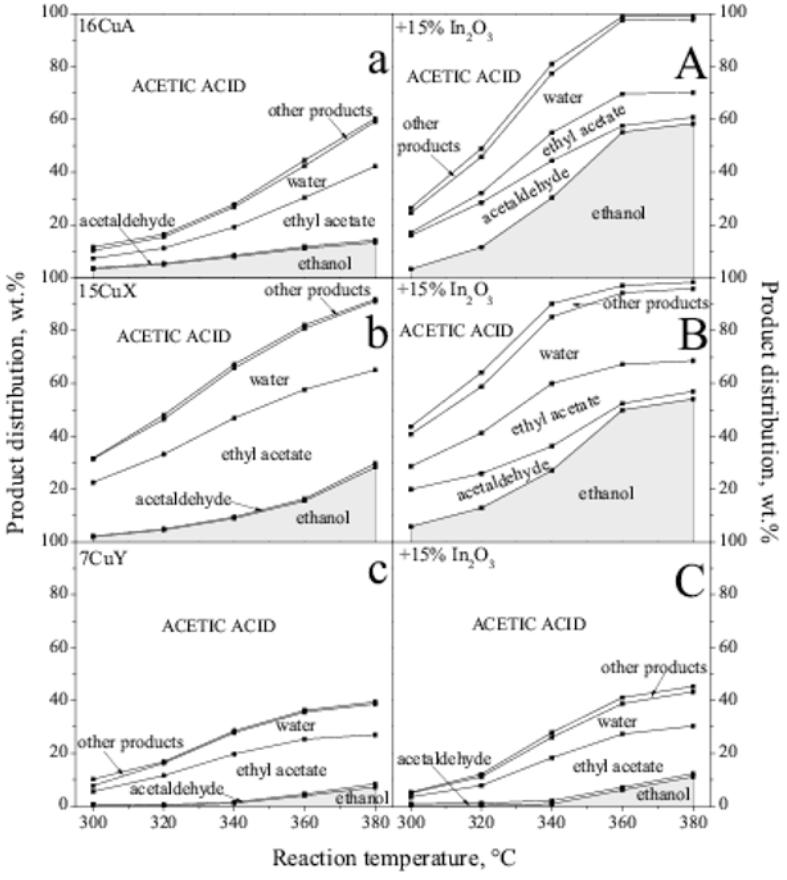

Figure 2. Product distribution of 16CuA (a,A), 15CuX (b,B), 7CuY (c,C) catalysts and (A, B, C) their composites with 15 wt.% In_2O_3 in the conversion of AA as function of reaction temperature at 21 bar in stacked area graphs. The partial pressures of AA and H_2 were 2.1 and 18.9 bar. The WHSV of AA was 1 h^{-1} (calculated for the CuZ mass only). The temperature was increased in 20°C steps. Data represent steady-state activities.

ethyl acetate being the main product. Such a direct reaction route to the valuable ester product can be economically more attractive and environmentally benign by replacing the conventional two-step process and eliminating the costly intermediate ethanol stage [17]. The copper catalysts prepared from zeolites A, X and P (Figs. 2a, 2b and 3b) have nearly the same Cu content and very similar aluminosilicate composition, but even so, show quite different activity and selectivity. The catalyst 14CuP, showing the highest activity among zeolites, is the most selective for ethanol formation at higher reaction temperature. The 7CuY catalyst is the most divergent zeolite among those studied because of solely stable structure under the pretreatment conditions. It shows the lowest activity having the lowest Cu-content, but at the same time containing the highest Brönsted acid site population in the non-damaged, intact faujasite micropore structure. This catalyst embodies a crystalline microporous HY support well permeable for the reactant without any damage of the microporous framework and has the biggest copper particles on the outer surface of the entire zeolite crystallites. However it seems to be a disadvantageous catalyst for the reaction investigated similarly to other thermally stable Cu-zeolites and unlike thermally unstable, destructed forms (Cu-A, -X and -P).

3.3. Conversion of the carboxylic acid over the In doped Cu-catalysts

When fatty acids of longer chains, e. g. OA, were reduced over the same catalysts, the addition of In_2O_3 to the catalyst drastically increased the conversion and the yield of octanol (Fig. 3a-A) [15]. While using AA as a reactant, the indium doping changed mainly the selectivity, but not the conversion (Fig. 3b-B), with exception of 16CuA, where In_2O_3 admission (Fig. 2a-A) also increased drastically the activity. The appearance of high concentration of acetaldehyde at lower conversions became important and the ethyl acetate yield was significantly lower. The product distribution could be hardly influenced by increasing the amount of the In_2O_3 modifying agent from 5 to 36 wt.%. This was not the case if the reactant was either OA [15] or AA over CuA. When

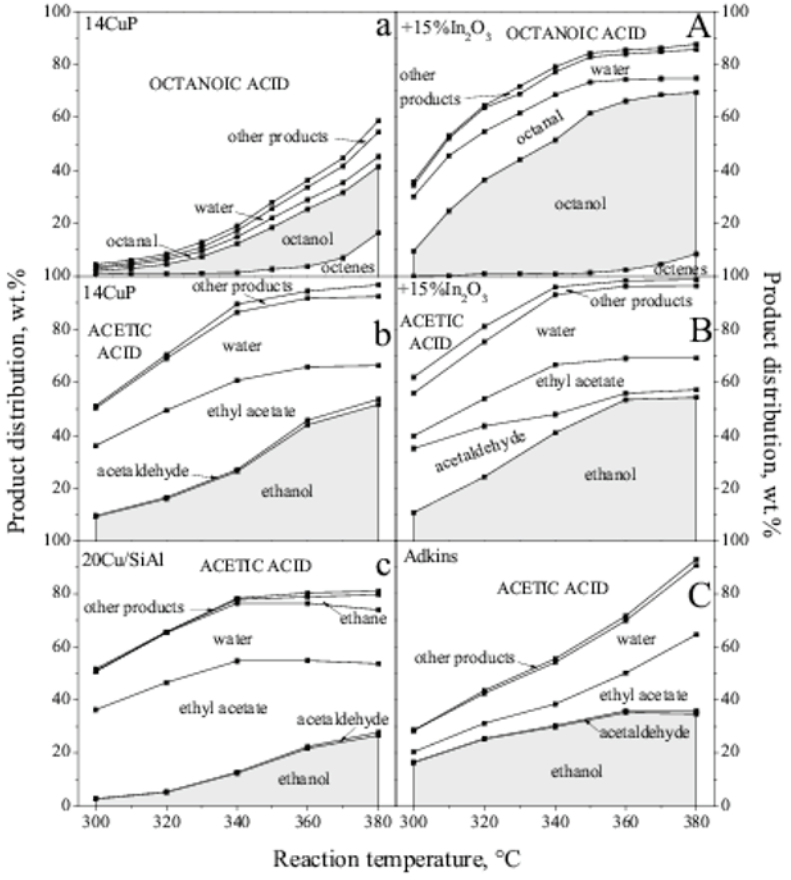

Figure 3. Product distribution of 14CuP (a,A) converted OA, 14CuP (b,B), 20Cu/SiAl (c) and conventional Adkins catalysts (C) converted acetic acid under conditions applied in Fig. 2. Fig. 3A and B show the effects of 15 wt.% In_2O_3 admission.

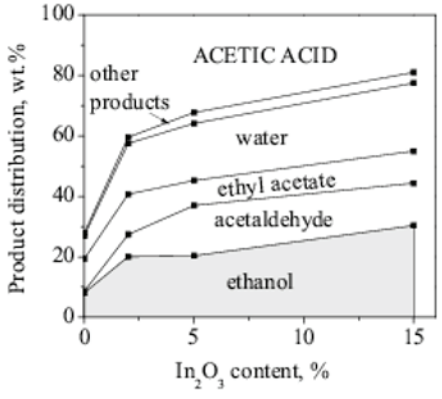

Figure 4. Comparison of 16CuA catalysts with various amounts of In_2O_3 admission in the hydroconversion of AA at 340°C and 21 bar. The partial pressures of AA and H_2 were 2.1 and 18.9 bar. The WHSV of AA was 1.0 h^{-1}.

comparing the 16CuA composite catalysts doped with various amounts of In_2O_3, the hydroconversion of AA at 340°C showed (Fig. 4) continuous, but weak increase of the overall activity and the ethanol yield between 2 and 15 wt.% In_2O_3.

However the greatest change took place at low loading, below 2 wt.%, suggesting that indium was effective already at low concentration. Catalyst 7CuY showed exceptional behavior compared with aluminium-rich zeolites (A, X, P), because In-doping could hardly influence its activity and product distribution (Fig. 2c-C). Unlike ethanol, the octanol can be in part dehydrated to olefins over CuP catalyst (Fig. 3a-A). The octyl octanoate formation was not significant but important octanal production could be observed. The octanol from OA and the ethanol from AA appeared together with the aldehydes at lower reaction temperature and conversions. The In_2O_3 additive mitigated the octene or ethyl acetate formation catalyzed by Brönsted acid sites and brought about higher yields of aldehydes from both carboxylic acids. Although a blocking effect of indium doping on acid sites could be recognized, the main effect should be a drastic quality change of the active metal surface in the presence of metallic indium, producing higher yields of the least reduced product, aldehydes (*e.g.* see Figs. 3A and 3B) at lower reaction temperature.

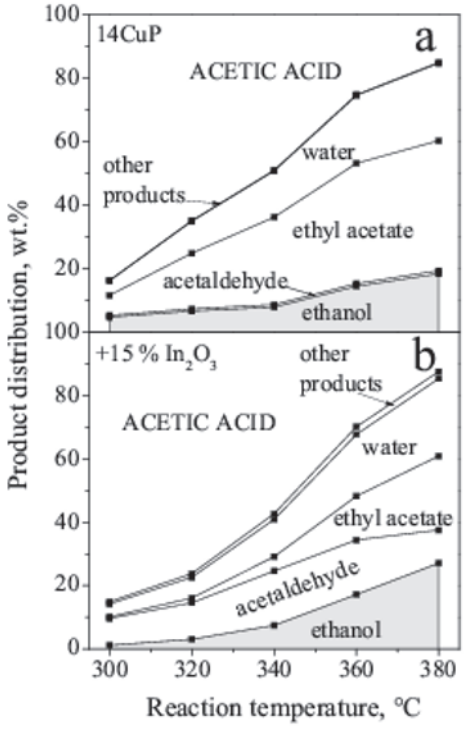

Figure 5. Product distributions of 14CuP (a) and $15In_2O_3$/14CuP (b) catalysts in the conversion of AA as function of reaction temperature at 21 bar. The partial pressures of AA and H_2 were 2.1 and 18.9 bar. The WHSV of AA was 3 h^{-1}.

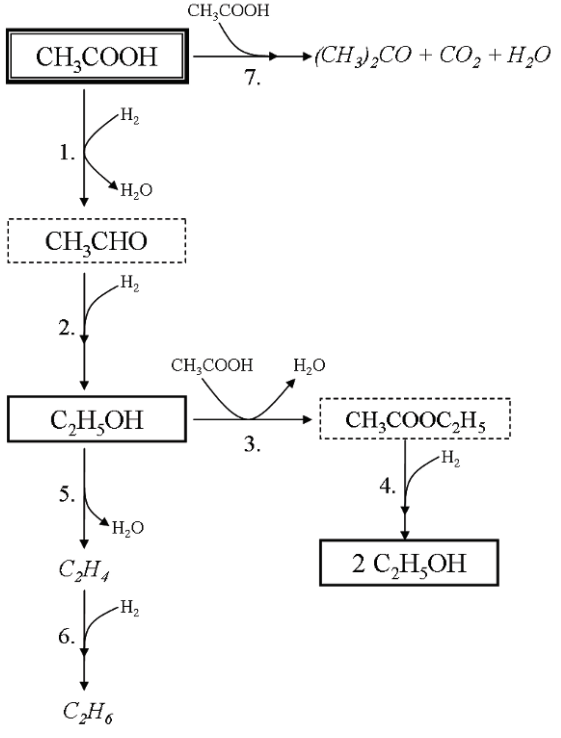

Scheme 1. Schematic diagram of reactions involved in the conversion of acetic acid on the base of the detected products.

The modification by indium changes the hydrogenation activity of the copper catalyst that is reflected in the appearance of less reduced compounds, aldehydes, in a relatively higher concentration in the product mixture (Figs. 2A-2B and 4A-4B). The acetaldehyde yield increased at the expense of the ethyl acetate yield. This selectivity change is more pronounced at lower temperatures. It is an exciting observation that the monometallic destructed zeolite catalysts, having lower activity without indium doping (16CuA with AA or 14CuP with OA, cf.: Fig. 2a-A or Fig. 3a-A), show highly increased hydroconversion activity following the In_2O_3 admission. In the systems giving a higher conversion before In doping (15CuX or 14CuP with AA, cf.: Fig. 2b-B or Fig. 3b-B) only the selectivity is changed.

3.4. Effects of reaction parameters

Fig. 5 shows the product yields and selectivities as a function of the reaction temperature under higher weight hourly space velocity (3 h^{-1} instead of 1 h^{-1}) resulting in lower conversions. The total conversion changed about linearly with the temperature in the full temperature range. The In_2O_3 additive did not show significant effect on the total conversion under this condition however, it decreased the yield of ethyl acetate and increased the yield of acetaldehyde and ethanol. Ethyl acetate can be formed from the reactant AA and the product ethanol by Fischer esterification. The Cu_2In alloy seemed to be showing less activity than pure copper in the second hydrogenation reaction step to ethanol, resulting in higher acetaldehyde (an intermediate product) yields, and be more active in ester hydrogenation (see in Scheme 1, where all the reactions responsible for the found products are summarized).

The AA conversion to ethanol and ethyl acetate increases roughly linearly with increasing hydrogen partial pressure over 14CuP and $15In_2O_3$/14CuP composite catalysts (Fig. 6) similarly to the conversion dependence of octanoic acid. It can be understood that high H_2 partial pressures do not favor the accumulation of acetaldehyde, an intermediate on the consecutive reaction pathway to alcohol, over the In doped sample. The acetaldehyde yield is the highest at lowest hydrogen partial pressures (at low conversions); it increases as the hydrogenation activity is suppressed, for instance, by an increased AA coverage (higher AA partial pressures) (see in Fig. 7). The found dependence of activity on the reactant partial pressures is in line with the Langmuir-Hinshelwood type kinetics and mechanism.

As expected the ethyl acetate selectivity responded also to the water content of the reactant mixture. As the water (which is always present in the light biomass-derived liquors) content of the feed was increased

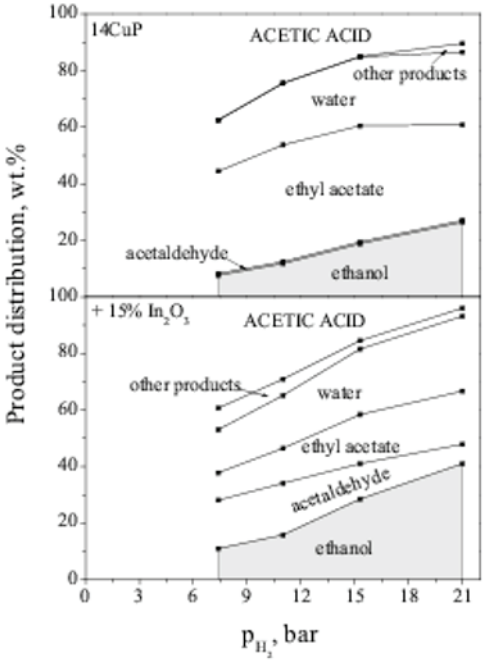

Figure 6. Product distribution of 14CuP and 15In_2O_3/14CuP catalysts in the conversion of AA/H_2/He mixture as function of hydrogen partial pressure at 21 bar total pressure and 340°C. The WHSV of AA was 1.0 h^{-1}. Constant partial pressure of AA was 2.1 bar. Hydrogen partial pressure was changed by changing the H_2/He ratio.

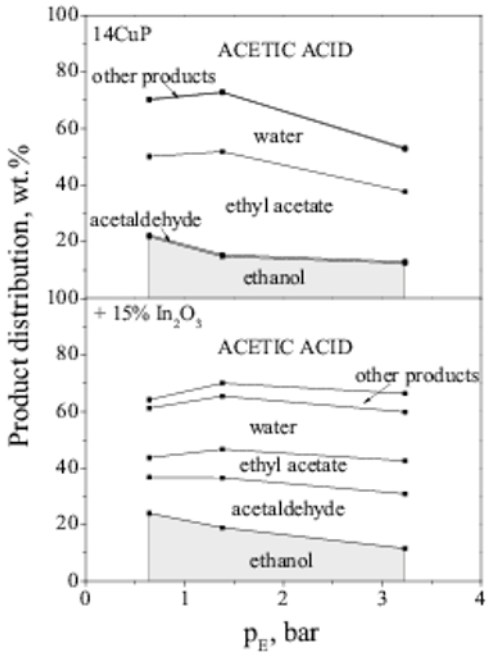

Figure 7. Product distribution of 14CuP and 15In_2O_3/14CuP catalysts in the conversion of AA/H_2/He mixture as function of AA partial pressure at 21 bar total pressure and 340°C. The WHSV of AA was 1.0 h^{-1}. Constant partial pressure of H_2 was 11 bar. The AA partial pressure was changed by changing the AA/He ratio.

(equal amount of water added to the acetic acid reactant) at 340°C over 15In_2O_3/14CuP composite catalyst, the selectivity of the aldehyde (15 → 25%) and the alcohol (60 → 64%) increased at the expense of the ethyl acetate selectivity (24 → 7%). Although the esterification can be suppressed by addition of water, as observed, bearing in mind the process economy other solutions are searched to increase the alcohol yield. It is a matter of course if the reduction of the catalyst acidity has positive effect.

Combining relatively simple pyrolytic (or biochemical) and catalytic technologies, bioethanol and chemicals, such as acetaldehyde and ethyl acetate, can be obtained from biomass, *e.g.* lignocellulosic raw material.

4. Conclusions

Small copper particles can be generated on amorphous aluminosilicate by dehydration/H_2-reduction of low-silica Cu-zeolites. The obtained Cu/aluminosilicate preparations have high activity and selectivity in the hydroconversion of biomass-derived carboxylic acids to alcohols, aldehydes and esters. The catalytic properties were shown to depend on the original zeolite structure. Hydrogenation activity and selectivity of the supported Cu/aluminosilicate catalysts can be significantly modified by In addition; the copper-indium alloy phase obtained has a moderated hydrogenation activity, permitting the accumulation of the acetaldehyde intermediate in the product mixture. The reaction parameters, which are favouring ethanol or ethyl acetate formation, are diametrically opposite.

Acknowledgements

The authors wish to express their appreciation to Mrs. Ágnes Farkas Wellisch for her technical assistance. Thanks is due to the Hungary-Slovakia Cross-border Co-operation Programme (Project registration number: HUSK/1101/1.2.1/0318) for supporting this research.

References

[1] G.W. Huber, S. Iborra, A. Corma, Chem. Rev. 106, 4044 (2006)

[2] D. Kubicka, Collect. Czech. Chem. Commun. 73, 1015 (2008)

[3] S.N. Naik, V.V. Goud, P.K. Rout, A.K. Dalai, Renew. Sust. Energ. Rev.14, 578 (2010)

[4] H.N. Chang, N.J. Kim, J. Kang, C.M. Jeong, Biotechnol. Bioproc. E. 15, 1 (2010)

[5] M.T. Holtzapple, C.B. Granda, Appl. Biochem. Biotech. 156, 525 (2009)

[6] V. Pham, M.T. Holtzapple, M. El-Halwagi, J. Ind. Microbiol. Biot. 37, 1157 (2010)

[7] T. Turek, D.L. Trimm, Catal. Rev. Sci. Eng. 36, 645 (1994)

[8] D.S. Brands, E.K. Poels, A. Bliek, Appl. Catal. A 184, 279 (1999)

[9] C.B. Granda, M.T. Holtzapple, G. Luce, K. Searchy, D.L. Mamrosh, Appl. Biochem. Biotech. 156, 537 (2009)

[10] W. Rachmady, M.A Vannice, J. Catal. 192, 322 (2000)

[11] W. Rachmady, M.A Vannice, J. Catal. 207, 317 (2002)

[12] W. Rachmady, M.A Vannice, J. Catal. 208, 158 (2002)

[13] W. Rachmady, M.A Vannice, J. Catal. 208, 170 (2002)

[14] W. Rachmady, M.A Vannice, J. Catal. 209, 87 (2002)

[15] Sz. Harnos, Gy. Onyestyák, J. Valyon, M. Hegedűs, Z. Károly, in: M. Derewinski, et al. (Eds.), Proc.10th Pannonian Int. Symp. Catal. Krakow (Polish Zeolite Association and Catalysis and Surface Chemistry, Kraków, 2010) 334

[16] B.D. Cullity, Elements of X-ray Diffraction, 2nd edition (Addison-Wesley Publ. Co. Reading, MA, USA, 1978)

[17] M.P. Atkins, Top. Catal. 24, 185 (2003)